THE ASTROPHYSICAL JOURNAL, 423:L35–L38, 1994 March 1


# WAVELENGTH-DEPENDENT KINEMATICS IN THE DUSTY INCLINED GALAXY NGC 2146

F. PRADA,[1] J. E. BECKMAN,[2] C. D. MCKEITH,[1] J. CASTLES,[1] AND A. GREVE[3]

*Received 1993 June 28; accepted 1993 December 3*


## ABSTRACT

We present measurements of the apparent rotation curves of the dusty inclined spiral NGC 2146 taken using conventional long-slit spectroscopy in the red and near-infrared. The curve measured in Hα emission shows, with respect to that observed in [S III] λ9069, a series of dips in velocity which coincide in positions with dips in the intensity of Hα, and with the dust lanes evident in broad band images. A more detailed quantitative comparison, including a previously published velocity curve in Brγ (Hutchings et al. 1990), using a schematic model, supports the hypothesis that dust is causing the Hα/[S III] discrepancies and highlights the need to measure rotation curves of inclined galaxies as far into the infrared as techniques permit. The λ9069 [S III] emission reveals a zone in expansion at 190 pc from the nucleus (previously detected in Brγ but at lower spectral resolution and with consequently limited velocity diagnostics) whose kinematics and energetics are well explained in terms of an expanding "superbubble" due to a starburst. Finally we suggest, from the invariance of the velocity curve with wavelength at nucleocentric radii greater than ~1500 pc that our observations imply very limited observable dust extinction in the outer parts of the disk of NGC 2146.


*Subject headings:* galaxies: individual (NGC 2146) — galaxies: ISM — galaxies: kinematics and dynamics — stars: formation

## 1. INTRODUCTION

Using near-infrared lines, we here investigate the effects of dust on the observed kinematics of the SB II peculiar galaxy NGC 2146 (Sandage & Tammann 1987), which is a highly inclined spiral with a prominent dust lane (Fig. 1 [Pl. L2]). De Vaucouleurs (1950) explains the projected geometry of the spiral pattern by the presence of a third arm inclined with respect to the principal plane of the galaxy and responsible for the strong absorption crossing the main body. The central regions of NGC 2146 are dusty and highly obscured. The visual extinction, toward the nucleus, has been estimated at 5–6 mag (Keel 1985; Benvenuti, Capaccioli, & D'Odorico 1975; Hutchings et al. 1990). From the regularity of the velocity field at different slit position angles, Benvenuti et al. (1975) showed there are no large-scale radial motions and inferred a mass of $4.6 \times 10^{10}\ M_{\odot}$ within 80″ of the nucleus. The CO velocity field is quite regular and shows a large velocity gradient of 0.2 km $s^{-1}$ $pc^{-1}$, which is steeper than the value measured in Hα (Jackson & Ho 1988), a difference almost certainly due to extinction effects. The CO intensity map agrees very well with the radio continuum map (Kronberg & Biermann 1981) which, unlike the optical, shows a remarkable degree of symmetry: the center of the radio continuum emission is hidden optically behind strong dust absorption. Kronberg & Biermann (1981) suggested that the radio emission is indicative of a young massive starburst and traces supernova events. Infrared images and colors indicate the existence of a significant population of hot young stars in the central region of the galaxy (Hutchings et al. 1990). From the Hα flux, Young, Kleinmann, & Allen (1988) inferred that nearly 40% of the radiation from the galaxy is due to OB stars. NGC 2146 has very active star formation and high dust content, and in this sense it is a typical IR-luminous galaxy.

The present observations were aimed at elucidating the kinematics within the inner 30″ of the galaxy, corresponding to some 2 kpc at its distance of 14.5 Mpc (Benvenuti et al. 1975). As we will see below, the use of the near-IR not only sharpened our understanding of the inner dynamics of the galaxy but also revealed an interestingly well defined direct kinematic observation of the effect of the starburst.

## 2. OBSERVATIONS AND DATA REDUCTION

The data were obtained in 1990 January with the ISIS spectrograph (Unger et al. 1988) on the 4.2 m WHT Telescope of the RGO facility at the Observatorio del Roque de los Muchachos, La Palma. Long-slit spectra were taken with the red arm of the ISIS spectrograph with a 1180 × 800 pixel CCD chip. The spectral dispersion was 0.73 Å $pixel^{-1}$. The 300 μm entrance slit width gave an angular resolution of 1.″5, slightly undersampling the 1″ seeing. The spectra of NGC 2146 were obtained placing the slit at a p.a. 128° through the nucleus and cutting the dense dust lane located in the NW region of the galaxy (Fig. 1). Two spectral images were recorded: one centered on Hα, including the [N II] λλ6548, 6584 lines and the [S II] λλ6717, 6784 lines; and another in the near-infrared wavelength region, including the Ca II IR triplet lines and the [S III] λ9069 lines. The exposure times were 1800 s for all the frames. Image reduction and analysis was performed using the UK STARLINK image processing package FIGARO (Shortridge & Bridger 1987) and DIPSO (Howarth 1987) for the flat-fielding and sky line subtraction. Given the limited spatial extent of NGC 2146 we were able to subtract the sky lines in both wavelength regions from sky spectra obtained at the ends of the slit. Wavelength calibrations were performed with CuAr arc spectra using the ARC2D calibration program. The peak velocities and intensities of the spectral lines were determined by fitting Gaussians with the LONGSLIT program for the analysis of calibrated long slit spectra. The

[1] Department of Pure and Applied Physics, Queen's University of Belfast, Belfast BT7 1NN, Northern Ireland.
[2] Instituto de Astrofisica de Canarias, E-38200 La Laguna, Tenerife, Spain.
[3] Instituto de Radio Astronomia Milimetrica, Nucleo central, Avd. Divina Pastora 7, 18102 Granada, Spain.

PLATE L2

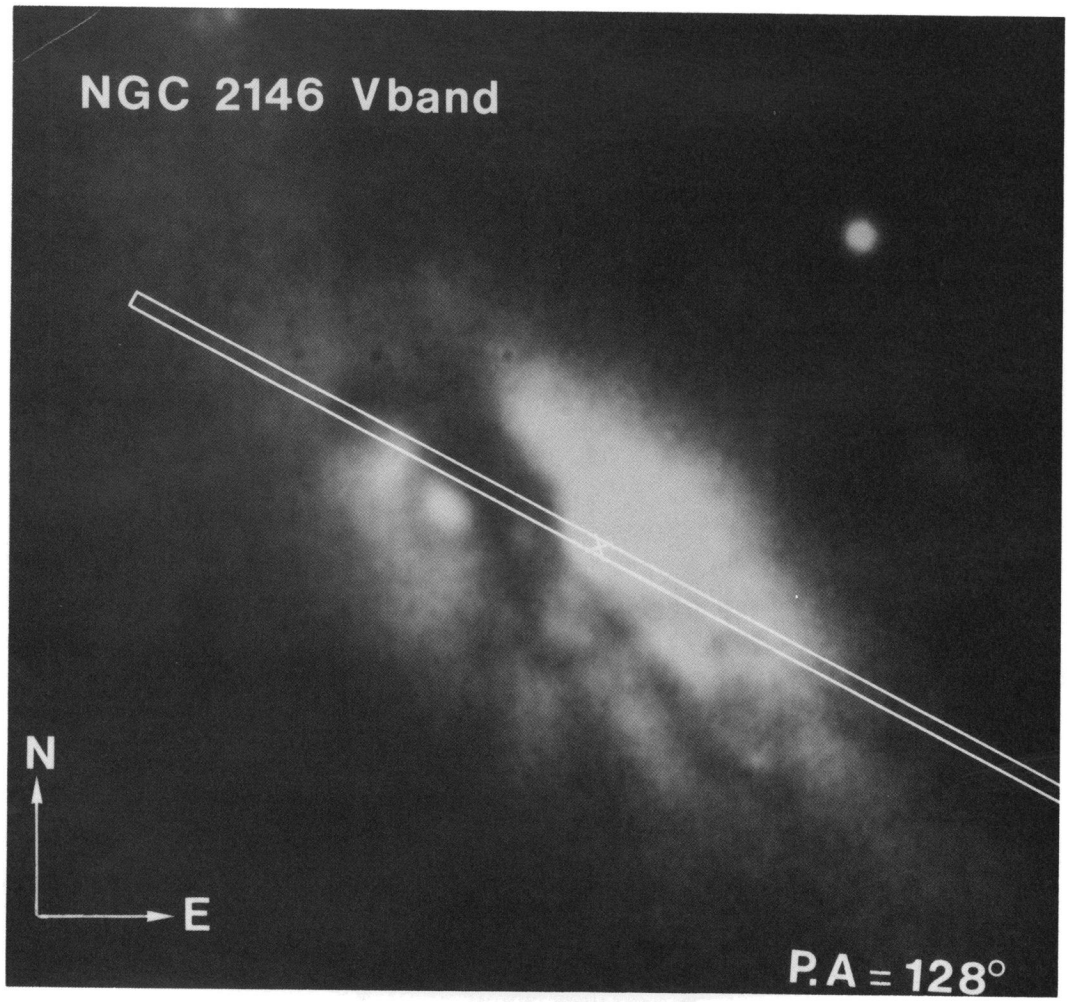


FIG. 1.—*V*-band CCD image of NGC 2146 taken with the JKT 1 m telescope, La Palma. The slit through the nucleus, along p.a. 128°, cuts the dust lane to the NE, where we see heavy dust obscuration (1 mm on the plate is 0".9, or 63 pc).

PRADA et al. (see 423, L35)

velocity errors were no more than 10 km s$^{-1}$. Both programs are in the TWODSPEC package (Wilkins & Axon 1991), implemented in the FIGARO package.

## 3. RESULTS

### 3.1. *Wavelength-dependent Kinematics*

We compare in Figure 2 the rotation curves of NGC 2146 at p.a. 128° in emission lines at different wavelengths: Hα, [N II] λ6584, and [S III] λ9069. At the position where the slit crosses the dust lane (the zone between 8″ and 20″ to the NW of the nucleus, see Fig. 1) we see differences in velocities at different wavelengths due to the effect of extinction as we discuss below in a simple model.

### 3.2. *Kinematics and Extinction*

We can use the measured differences in the observed rotation curves in the three emission lines we observed, as well as, Brγ taken from Hutchings et al. (1990), displayed in Figure 2, to show via a simple model that dust extinction is the probable cause of their divergence, notably in the zone between 8″ and 20″ to the NW of the nucleus. Selecting a point 10″ from the nucleus at this side where, as seen on Figure 1, the slit is in fact crossing a strong dust lane, we measure for the three emission lines the differences between the systemic velocity of the galaxy (916 ± 20 km s$^{-1}$, in good agreement with the value 909 ± 19 km s$^{-1}$ given by Benvenuti et al. 1975) and the observed radial velocities, with values presented in the table (See Fig. 3).

Any attempt to model the effect of the dust obscuration must deal with an unknown geometry as well as an unknown true rotation curve. For simplicity we choose an exponential distribution of dust with radius, and taking the effective radius of emission, $r_{em}(\lambda)$, as that where the dust optical depth at wavelength $\lambda$ is close to unity, we derive the form

$$r_{em}(\lambda) = \alpha \ln A_\lambda + \beta$$

for the dependence of $r_{em}(\lambda)$ on the extinction $A_\lambda$, where $\alpha$ and $\beta$ are constants. In Figure 3 we plot $r_{em}(\lambda)$ against $\ln A_\lambda$ and find an acceptable linear fit to the data, which suggests that the dust is a probable cause of the velocity differences observed. To obtain the fit we began by assuming that the Brγ curve (Hutchings et al. 1990) represents velocities very close to those which would be measured along the major axis in the absence of dust. The reduced projected velocities for [S III] and Hα in the table are the results of geometrical projection imposed by the dust, with the lines of sight achieving only partial penetration, as illustrated in Figure 3. The distance from the nucleus to the point on the major axis from which we assume the Brγ radiation comes, is 700 pc, corresponding to 10″, for a distance to NGC 2146 of 14.5 Mpc (Benvenuti et al. 1975). At this radial distance from the nucleus the rotation curve is still rising, according to the Brγ data, which we can use to estimate the effective nucleocentric distances from which the [S III] and Hα, seen projected at 10″, should be coming. These distances are 1200 pc and 1475 pc, respectively. The visual dust optical depth, $A_v$, given by this model corresponding to the emission point from which the Brγ is received is close to 10 mag.

We make no major claim for this modeling exercise, based as it is on a number of assumptions which are not fully supported; it should be treated strictly as semiquantitative evidence for the view that dust rather than, for example, variation in excitation conditions is probably responsible for the velocity differences measured. This conclusion is further strongly supported by the fact that the Hα and [N II] λ6584 curves in Figure 2, follow each other perfectly within the limits of measurement errors, as expected for lines close in wavelength where dust was the important factor rather than difference in

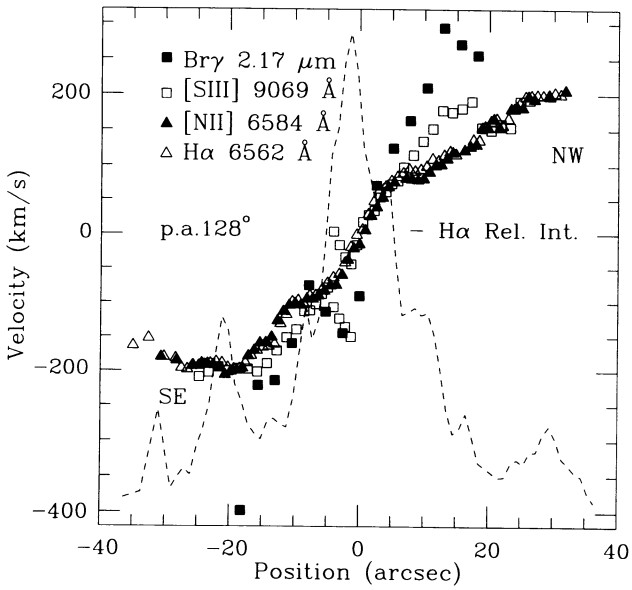


FIG. 2.—Measured radial velocities in Hα, [N II] λ6584, and [S III] λ9069, along an axis at p.a. 128°, of NGC 2146 (see Fig. 1), compared with the curve for Brγ taken at slightly different position angle (p.a. 135°) by Hutchings et al. (1990). Velocity differences between the Brγ, [S III] velocities and the Hα/[N II] velocities are greatest where extinction is clearly reducing the Hα intensity, i.e., in zones of maximum dust concentration (NW of the galaxy). The errors in velocity were no greater than 5 km s$^{-1}$ (except for Brγ). Note also the noncircular motions in [S III] (and Brγ), 2.″7 to the SE of the nucleus, due to an expanding starburst zone (see text) (1″ = 70 pc).

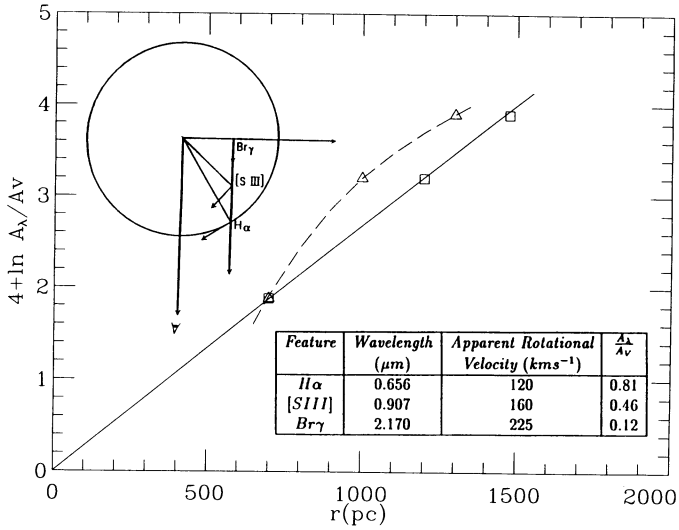


| Feature | Wavelength (μm) | Apparent Rotational Velocity (kms$^{-1}$) | $\frac{A_\lambda}{A_v}$ |
|---|---|---|---|
| *IIα* | 0.656 | 120 | 0.81 |
| *[SIII]* | 0.907 | 160 | 0.46 |
| *Brγ* | 2.170 | 225 | 0.12 |

FIG. 3.—Plots of the logarithm of the relative coefficient $A_\lambda/A_v$ at wavelength $\lambda$ against the computed galactocentric weighted distance $r$, for emission at that wavelength, based on models with two kinematic schemes: (a) A constant rotational velocity (*dashed line, triangular symbols*) and (b) rotational velocity varying with radius according to the rotation measured in Brγ, shown in Fig. 1 (*continuous line, square symbols*). The model fits to the data used the circular projection scheme shown in the inset, where the observed Brγ, [S III], and Hα emissions come from increasing values of $r$, according to dust penetration depth. The table compares observed projected circular velocities in three emission lines for the point 10″ to the NW of the nucleus and tabulates the relative extinction coefficients which were used in the schematic dust model.

excitation. Further, in Figure 2, we note that the relative intensity of Hα, at some places along the slit, falls due to heavy obscuration, where the dust lane is located (Fig. 1). This phenomenon was noticed by Hutchings et al. (1990). They described the overall Hα velocity field in NGC 2146 as that of a regular rotating disk but pointed out that dips in the velocity curve occur at positions where the intensity of the Hα is reduced, ascribing this to dust extinction.

There are two other notable kinematic features in Figure 2. Between some 18″ and 24″ from the center to the NW, there is a sudden dip in the rotation curve, in which [S III], Hα, and [N II] coincide in velocity. We can account for this by the presence of the "third arm" feature described in the introduction, which cuts the spectrograph slit in this region. This feature is characterized by exceptionally strong dust absorption as revealed in the $J$(1.95 μm) band (Hutchings et al. 1990), and we must assume that here the emission in all the lines is coming from near the front surface of the feature. Beyond some 20″ to the SE and some 24″ to the NW, we reach what must be the plateau of the true rotation curve for NGC 2146, finding no significant difference between [S III], Hα, and [N II] velocities in these regions. The simplest way to explain this is that there is very little dust affecting the projected rotational components beyond this point of the galactic disk, some 1500 pc from the center of the galaxy, a conclusion akin to that of a similar study due to Bosma et al. (1992) of NGC 891. Additional evidence, such as the absence of obvious dust in the $V$-band image (Fig. 1), the relative smoothness and flatness of the curves, and the approximate equality of the velocity moduli for the SE and NW "plateau" regions does point to a low dust solution for the outer disk, but there are still grounds for caution about this inference.

Further support for the hypothesis that dust absorption is the cause of the divergences between the rotation curves observed in the different emission lines comes from the rotation curve measured in the line of $^{12}$CO $J = 1 \rightarrow 0$ (Jackson & Ho 1988). The slope of this curve is a little steeper than that in Hα to the SE of the nucleus, but much steeper to the NW in the zone of the dust lane (Jackson & Ho 1988). This of course, is in accord with deeper dust penetration in CO as is the symmetry of the CO curve about the nucleus.

### 3.3. *Star Formation Activity*

NGC 2146 shows strong nonthermal radio continuum emission (Kronberg & Biermann 1981) and high *IRAS* FIR luminosity ($6.5 \times 10^{10}\ L_{\odot}$; Sanders et al. 1986) suggesting a young and strong starburst in which OB stars dominate the emitted luminosity. VLA radio continuum observations reveal, a population of ~20 point sources embedded in a diffuse nonthermal background (Glendenning & Kronberg 1986). These radio sources are probably supernovae (SNs) or young supernova remnants and appear equivalent to the sources found in M82 by Kronberg & Sramek (1985). The most intense radio emission in NGC 2146 forms a bar of dimension 40″ × 6″ elongated along p.a. 128°, and the peak of this radio emission forms the center of a barlike "triple" source suggesting a S shape at p.a. 105° (Kronberg & Biermann 1981).

Our [S III] λ9069 observations, along the p.a. 128°, show a double velocity structure centered 2.″7 (~190 pc) to the SE from the nucleus (Fig. 2). This is consistent with a large-scale expansion or "superbubble" due to supernova events, which cannot be seen in Hα or [N II] λ6584 (Fig. 2) because of dust extinction. This velocity expansion is not fully sampled in the Brγ rotation curve by Hutchings et al. (1990) due to the moderate velocity resolution (40 km s$^{-1}$), although we can in fact see a sharp velocity step in Brγ at the position of the superbubble in the [S III] rotation curve. The superbubble can be identified with one of the lobes of the S-shaped central barlike triple radio source described by Kronberg & Biermann (1981). A number of supernovae occurring frequently in an OB association may create a superbubble (Mac Low & McCray 1988), which is a large, thin shell of cold gas surrounding a hot pressurized interior. The superbubble detected here using [S III] λ9069 in NGC 2146 has an expansion velocity of ~60 km s$^{-1}$ and a radius ~140 pc deprojected using an inclination, $i = 65°$ (Benvenuti et al. 1975). The mechanical luminosity $L_{SN}$ of the superbubble and the dynamical time $t$ of the expansion can be estimated from its expansion velocity $v$ and Radius $R$, using the equations given by Mac Low & McCray ($L_{SN} \sim 3.6 \times 10^{26} n_0$ (cm$^{-3}$) $R_{pc}^2 V_{km\,s^{-1}}^3$; $t \sim 0.6\ R_{pc}/V_{km\,s^{-1}}$), where $n_0$ is the density of the medium in the bubble. For a value for $n_0$ of ~600 cm$^{-3}$ (Benvenuti et al. 1975) we find a luminosity due to supernovae $L_{SN} \sim 3 \times 10^{49}$ ergs yr$^{-1}$ and a dynamical time of 1.4 Myr. Assuming that a single SN deposits an energy of $10^{50}$ ergs in the ISM, we thus estimate a rate of ~0.3 SNs yr$^{-1}$, which is in reasonable agreement with a theoretical value of 0.1 SNs yr$^{-1}$ obtained using the FIR luminosity (SN rate = $0.2 L_{IR,11}$ yr$^{-1}$; Heckman, Armus, & Miley 1990). This fits Jackson & Ho's (1988) inference that the two galaxies have similar ratios of the total IR luminosity to the total $H_2$ mass, so the efficiency of star formation is as high in NGC 2146 as in M82.

## 4. IMPLICATIONS FOR EXTINCTION AND EXCITATION MEASUREMENTS

If our explanation of the rotation curve discrepances due to dust is correct, visual extinction in NGC 2146 cannot be derived as previously assumed by Young et al. (1988) from the [S III]/Hα intensity ratios because the photons which reach us are coming from different galactocentric radii as shown by their different rotation curves (Fig. 2). For the same reason, i.e., that emission in [S III] and Hα along the same line of sight may come from very different zones of the galaxy, the observed [S III]/Hα ratio cannot even be used reliably as an indicator of nebular excitation, as assumed by Kennicutt & Pogge (1990). Moreover, the Brγ/Hα ratio used by Hutchings et al. (1990) does not give a good estimate of the excitation either. In fact, we cannot get a reliable estimation of the $A_V$ value from line intensity ratios at different wavelengths. We would be on somewhat safer ground using line ratios at longer wavelengths, i.e., near-infrared lines. The same considerations apply to similar observations in comparable galaxies; Waller, Gurwell, & Tamura (1992), for example, use the Brγ/Hα ratio to estimate the extinction in M82. We know, from a comparison at the [S III] λ9069 rotation curve by McKeith et al. (1993) with that in Hα, that the near-infrared emission in M82 comes from radii much closer to the galactic center than the Hα and this geometrical displacement effect will be stronger still for the Brγ versus Hα curves. We therefore offer a warning that the use of intensity ratios without the corresponding kinematic data can lead to misleading estimates of extinction in the presence of dust, especially in inclined galaxies, and that even with the help of the kinematics, any result will be model dependent.

We are grateful for the help of D. Carter and other staff members of the Royal Greenwich Observatory at the Spanish

Observatorio del Roque de los Muchachos of the Instituto de Astrofisica de Canarias. We than E. Perez, J. M. Rodriguez Espinosa, J. M. Vilchez, B. Vila, J. Acosta, and especially Alicia Gordillo for valuable comments on the manuscript. F. Prada is the holder of a SERC research studentship, at QUB, under the IAC-SERC agreement.

## REFERENCES

Benvenuti, P., Capaccioli, M., & D'Odorico, S. 1975, A&A, 41, 91
Bosma, A., Byun, Y., Freeman, K. C., & Athanassoula, E. 1992, ApJ, 400, L21
de Vaucouleurs, G. 1950, Ann. d'Ap., 13, 362
Fisher, J. R., & Tully, R. B. 1976, A&A, 53, 397
Glendenning, B. E., & Kronberg, P. P. 1986, BAAS, 18, 1006
Heckman, T. M., Armus, L., & Miley, G. 1990, ApJS, 74, 833
Heiles, C. 1979, ApJ, 229, 533
Howarth, I. D. 1987, STARLINK User Note 50, Rutherford Appleton Lab.
Hunter, D. A., Gillet, F. C., Gallagher, J. S. Rice, W. L., & Low, F. J. 1986, ApJ, 303, 171
Hutchings, J. B., Neff, S. G., Stanford, S. A., & Unger, S. W. 1990, AJ, 100, 60
Jackson, J. M., & Ho, P. T. P. 1988, ApJ, 324, L5
Keel, W. C. 1984, ApJ, 282, 75
Kennicutt, R. C., Jr., & Pogge, R. W. 1990, AJ, 99, 61
Kronberg, P. P., & Biermann, P. 1981, ApJ, 243, 89
Kronberg, P. P., & Sramek, R. A. 1985, Science, 227, 28
Mac Low, M.-M., & McCray, R. 1988, ApJ, 324, 776
McKeith, C. D., Castles, J., Greve, A., & Downes, D. 1993, A&A, 272, 98
Rieke, G. H., Lebofsky, M. J., Thompson, R. L., Low, F. J., & Tokunaga, A. T. 1980, ApJ, 238, 24
Sandage, A., & Tammann, G. A. 1987, A Revised Shapley-Ames Catalog of Bright Galaxies (2d ed.; Washington: Carnegie Institution of Washington)
Sanders, D. B., Soifer, B. T., Neugebauer, G., Young, J. S., Matthews, K., & Yerka, J. 1986, ApJ, 289, 129
Shortridge, K., & Bridger, A. 1987, STARLINK User Note 40, Rutherford Appleton Lab.
Unger, S. W., Brinks, E., Laing, K. P., Tritton, K. P., & Gray P. M. 1988, Observers' Guide. Isaac Newton Group, La Palma, Version 2.0.
Waller, W. H., Gurwell, M., & Tamura, M. 1992, AJ, 104, 63
Wilkins, T. N., & Axon, D. J. 1991, STARLINK User Note 16.3, Rutherford Appleton Lab.
Young, J. S., Claussen, M. J., Kleinmann, S. G., Rubin, V. C., & Scoville, N. 1988, ApJ, 331, L81
Young, J. S., Kleinmann, S. G., & Allen, L. E. 1988, ApJ, 334, L63